

A Discrete Amphiphilic Organoplatinum(II) Metallacycle with Tunable Lower Critical Solution Temperature Behavior

Peifa Wei,[†] Timothy R. Cook,^{‡,||} Xuzhou Yan,[†] Feihe Huang,^{*,†} and Peter J. Stang^{*,‡}

[†]State Key Laboratory of Chemical Engineering, Department of Chemistry, Zhejiang University, Hangzhou 310027, P. R. China

[‡]Department of Chemistry, University of Utah, 315 South 1400 East, Room 2020, Salt Lake City, Utah 84112, United States

^{||}Department of Chemistry, University at Buffalo, 359 Natural Sciences Complex, Buffalo, New York 14260, United States

S Supporting Information

ABSTRACT: Oligo(ethylene glycol) (OEG)-decorated supramolecular assemblies are distinguished by their neutral character and macroscopic temperature-sensitive phase transition behavior. OEG functionalization is an emerging strategy to obtain thermoresponsive macrocyclic amphiphiles, although known methods organize the hydrophilic and hydrophobic segments by covalent bonding. Coordination-driven self-assembly offers an alternative route for organizing OEG-functionalized precursors into nanoscopic architectures, resulting in well-defined metallacycle cores surrounded by hydrophilic scaffolds to impart overall amphiphilic character. Here a tri(ethylene glycol)-functionalized thermosensitive amphiphilic metallacycle was prepared with high efficiency by means of the *directional-bonding approach*. The ensembles thus formed showed good lower critical solution temperature behavior with a highly sensitive phase separation and excellent reversibility. Moreover, the clouding point decreased with increasing metallacycle concentration and addition of K⁺.

The temperature-induced helix/coil transition of polypeptides is one of many examples of natural biomacromolecules undergoing dramatic conformational changes that result in new physiochemical properties.¹ These thermoresponsive natural materials motivate the design and development of artificial analogues, prompting both fundamental and applied research efforts.² These materials are soluble in solution below a certain temperature, known as the *lower critical solution temperature* (LCST). Above the LCST, increased aggregation results in turbidity. Materials that exhibit LCSTs are useful for molecular separation,³ smart surfaces,⁴ drug delivery,⁵ and sensors.⁶ These applications prompted the design of polymeric materials such as poly(*N*-isopropylacrylamide), which displays a LCST of ~32 °C in water.⁷ Non-polymeric LCST materials, such as those based on simple discrete organic molecules or macrocycles, are comparatively rare.⁸

Macrocyclic amphiphiles (MCAs), a class of fascinating macrocyclic molecules containing both hydrophilic and hydrophobic segments, can spontaneously aggregate to form multidimensional and hierarchical self-assemblies, driven by microphase separation of the hydrophilic and hydrophobic groups into ordered periodic structures, due to their mutual repulsion.⁹ Oligo(ethylene glycol)s (OEGs) have been widely used to

synthesize topologically controllable and diverse smart materials with fine-tuned thermoresponsiveness to external stimuli.¹⁰ A handful of thermoresponsive MCAs with covalently connected OEGs have been reported.¹¹ However, tedious multistep organic synthesis and purification processes are hallmarks of this approach. Supramolecular self-assembly provides an alternative way to realize thermal sensitivity in discrete architectures. The spontaneous formation of metal–ligand bonds is a valuable methodology to construct supramolecular coordination complexes.¹² This design strategy is particularly relevant for amphiphilic materials, as the core and periphery of the precursors and final metallacycles can be carefully controlled. The orientation and extent of functionalization can be tuned, along with the shape and dimensions of the internal cavity, providing facile routes toward amphiphilic metallacycles¹³ with thermoresponsiveness. Here the thermoresponsiveness afforded by OEG functionalities is preserved on a neutral hexagonal metallacycle core, resulting in an amphiphilic metallacycle with a LCST that is responsive to both metallacycle concentration and addition of K⁺.

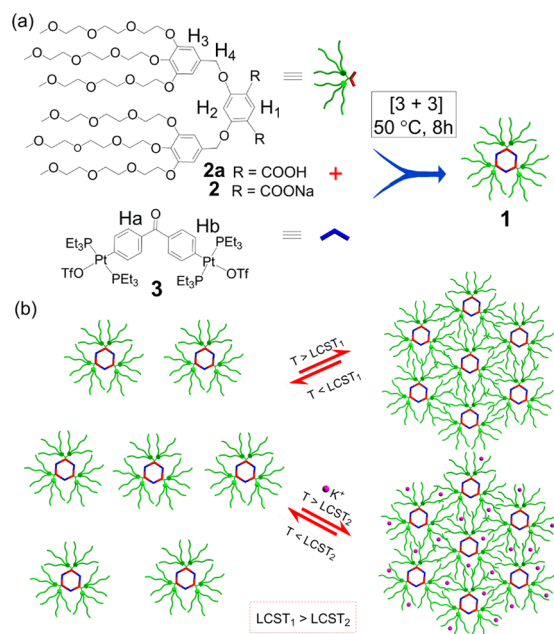
Our group reported a class of amphiphilic rhomboids comprising neutral metallacycle cores decorated with hydrophilic moieties, obtained via Pt–carboxylate bond formation.^{13b} Those systems demonstrated hierarchical self-assembly of dimensionally controllable nanostructures. Although that work pioneered a new route to synthesize amphiphilic metallacycles, functionalization of these amphiphilic metallacycles has not yet been reported. Our current efforts utilize the charge-neutral tri(ethylene glycol) (Tg) as a pendant group to impart temperature sensitivity into amphiphilic metallacycles.

The metallacycles were obtained via self-assembly reactions following the formation of a Tg chain-functionalized 120° dicarboxylate ligand, **2**. When this donor was mixed with a 120° organoplatinum(II) acceptor, **3**, in a 1:1 ratio in D₂O/acetone-*d*₆ at 50 °C for 8 h, a [3+3] self-assembly occurred to give amphiphilic metallacycle **1**, containing hydrophilic Tg chains around the hydrophobic core (Scheme 1a). The precursors **2** and **2a** were used as model compounds to evaluate how a cyclic structure affects the LCST of **1** relative to that of the free ligands. ¹H and ³¹P NMR analyses of the product supported the formation of hexagonal, three-fold-symmetric species. The ³¹P{¹H} NMR spectrum of **1** possessed a sharp singlet at

Received: September 10, 2014

Published: October 23, 2014

Scheme 1. (a) Self-Assembly of 2 and 3 To Give an Amphiphilic Discrete Organoplatinum(II) Metallacycle and (b) Cartoon Illustration of Its Thermosensitivity and Potassium Cation Responsiveness



~16.30 ppm with concomitant ^{195}Pt satellites ($J_{\text{Pt-P}} = 2310.5$ Hz), consistent with a single phosphorus environment (Figure 1b). This peak shifted upfield relative to that of acceptor 3 by ~2.94 ppm. Moreover, in the ^1H NMR spectrum of **1**, protons H_2 , H_3 , and H_4 on **1** showed downfield shifts compared with those of **2** (Figure 1d,e), in accord with coordination of the O-atom to the Pt centers. Electrospray ionization time-of-flight mass spectrometry (ESI-TOF-MS) provided further evidence for the formation of **1**. Three peaks were found to support the assignment of a [3+3] assembly (Figure 2), including those corresponding to an intact hexagonal core with charge states arising from the loss of counterions ($m/z = 1458.40$ for $[\text{M} + 2\text{Na} + \text{H} + \text{K} + \text{NH}_4]^{5+}$ (Figure 2a), $m/z = 1462.00$ for $[\text{M} + 2\text{Na} + \text{H} + \text{K} + \text{NH}_4 + \text{H}_2\text{O}]^{5+}$ (Figure 2b), and $m/z = 1817.45$ for $[\text{M} + 2\text{Na} + 2\text{NH}_4]^{4+}$ (Figure 2c). The Na^+ and K^+ ions were introduced as trace impurities either from the glass vessels used or from the addition of NH_4Cl to solutions of **1** to facilitate ionization. All the peaks were isotopically resolved and agreed very well with their calculated theoretical distributions.

With the amphiphilic metallacycle in hand, we investigated its thermoresponsive behavior. The long Tg chains of **2**, **2a**, and **1** rendered them fully soluble in aqueous solution at 25.0 °C (1.00 mM). Clear aqueous solutions of **1** turned turbid upon mild heating and returned to clear upon cooling. This reversible transformation was the first evidence that **1** exhibited LCST behavior in an aqueous solution. For model compound **2a**, an aqueous solution at 1.00 mM became opaque until the temperature exceeded 80.0 °C, indicative of a LCST that is too high for practical applications. Model compound **2** showed no LCST behavior, attributed to its high solubility in water precluding aggregation. These control experiments reveal the importance of the metallacycle core in achieving reversible LCST behavior. The combination of the hydrophilic OEGs and hydrophobic hexagonal scaffolds is necessary to impart the amphiphilic behavior that is the foundation for the thermal responsiveness.

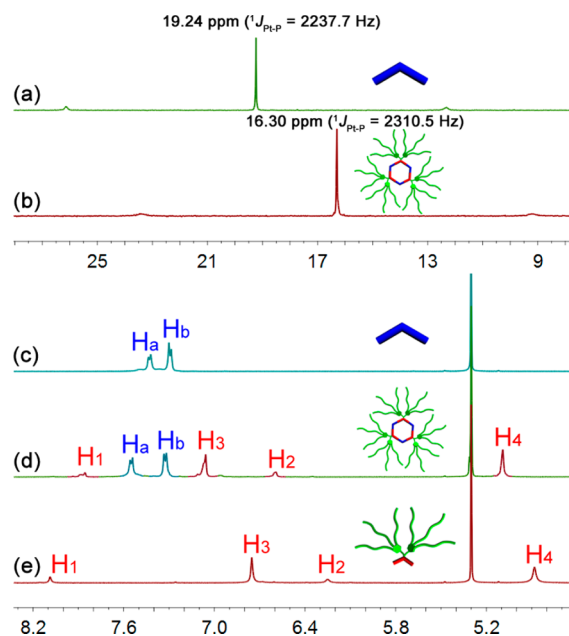


Figure 1. (a,b) ^{31}P NMR and (c–e) partial ^1H NMR spectra (CD_2Cl_2 , 293 K) of free building blocks **2** (e) and **3** (a,c), and hexagonal metallacycle **1** (b,d).

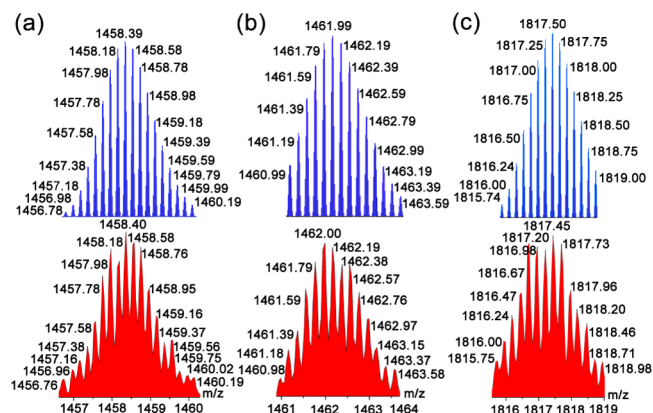


Figure 2. Experimental (red) and calculated (blue) ESI-TOF-MS spectra of **1**: (a) $[\text{M} + 2\text{Na} + \text{H} + \text{K} + \text{NH}_4]^{5+}$, (b) $[\text{M} + 2\text{Na} + \text{H} + \text{K} + \text{NH}_4 + \text{H}_2\text{O}]^{5+}$, and (c) $[\text{M} + 2\text{Na} + 2\text{NH}_4]^{4+}$.

It is well known that the thermal sensitivity of OEGs results from reversible disruption of H-bonds between OEG chains and surrounding water molecules.¹⁰ Below the clouding point (T_{cloud}), H-bonding interactions between the Tg chains of **1** and exogenous water molecules dominate, whereas the Tg chains become non-polar and intra-/intermolecular H-bonding interactions increase above T_{cloud} . Thus, at high temperatures, the surface of **1** is hydrophobic, promoting aggregation of the Tg chains ultimately into micellar structures that induce light scattering. This scattering provides a means to evaluate the T_{cloud} of **1**, namely by investigating the change in transmittance at 700 nm with a temperature-controlled UV/vis spectrometer. The optical transmittance at 700 nm was used for T_{cloud} measurements because the transmittance change at this wavelength was clearly noticeable. Figure 3a shows the temperature dependence of the light transmittance of aqueous solutions of **1**. In all cases the transmittance decreased drastically in response to a minor change in temperature around T_{cloud} , indicating a highly sensitive phase separation. We also investigated the reversibility of this

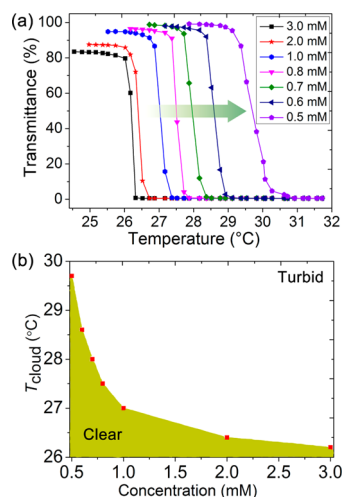


Figure 3. (a) Transmittance as a function of temperature for aqueous solutions of **1** with different concentrations. Heating rate = 0.200 K min^{-1} . (b) Concentration dependence of the clouding point of **1** in aqueous solution. $c = 3.00$ mM.

LCST system. Upon cooling to 25.0 °C, the cloudy 3.00 mM solution became transparent, exhibiting a dehydration/hydration transition. The solution of **1** showed no signs of fatigue under modest heating/cooling cycling, demonstrating that this process was reversible (Figure 4a). Figure 3b shows that a stepwise

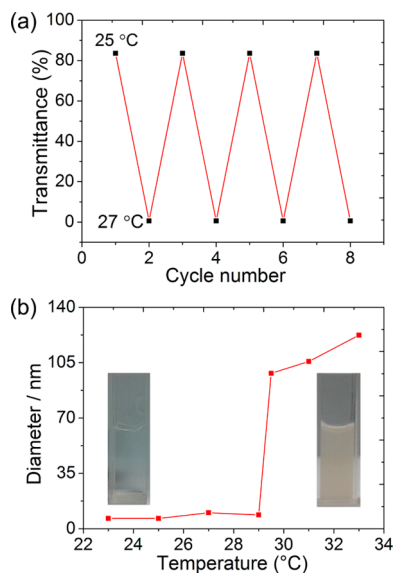


Figure 4. (a) Change in transmittance of 2.00 mM **1** when cycling between 25.0 and 27.0 °C. (b) Dependence of hydrodynamic diameter of aggregates in 0.500 mM solution of **1** on temperature. Insets: Photographs of the solutions below and above T_{cloud} .

decrease in $[\mathbf{1}]$ from 3.00 to 0.500 mM leads to a sharp increase of T_{cloud} , indicating that the LCST behavior depends on the concentration of the metallacycle. This trend is consistent with that observed for other molecules that show LCST behavior.^{10a}

The first step in determining the sizes of the supramolecular aggregates as the temperature was changed was to establish the monomeric metallacycle dimensions. A simulated molecular model of **1**, optimized with the Molecular Mechanics Universal Force Field, indicated a planar hexagonal framework with exohedral functionalization of the pendent Tg units and an

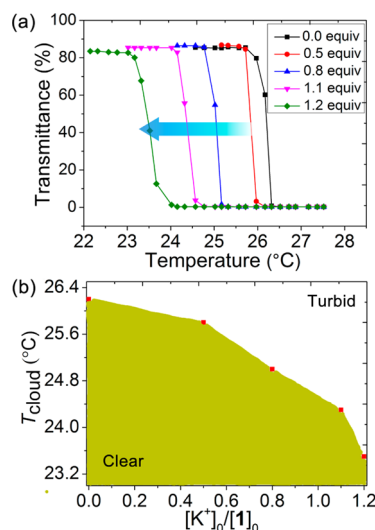


Figure 5. (a) Transmittance as a function of temperature for different molar ratios of **1** and K^+ at a heating rate of 0.200 K min^{-1} . (b) Dependence of the clouding point on the molar ratio of **1** and K^+ in aqueous solution. $c = 2.00$ mM.

extended length of 5.62 nm (Figure S10). Transmission electron microscopy (TEM) was used to reveal changes in the microstructures induced by the LCST behavior (Figure S11). Spherical micellar structures of **1** were observed at 0.500 mM. The diameters were ~ 7.00 nm below 29.0 °C. When the solution was heated to 30.0 °C, the nanoparticles increased to ~ 100 nm on average. This aggregation process is consistent with $T_{\text{cloud}} = 29.0$ °C, matching the value determined by absorption techniques (Figure 3b). The TEM results indicate that solutions were populated with monomers below the LCST, as the mean diameter of the aggregates was on par with the size of a discrete hexagon. This monodispersity of **1** is reasonable because its hydrophilicity is too high compared with its hydrophobicity.^{11a,12e} The aggregation process of **1** in aqueous solution was further evidenced by dynamic light scattering. At 23.0–29.2 °C, the average hydrodynamic diameter (D_{H}) was ~ 9.00 nm (Figure 4b). When the temperature was raised above T_{cloud} (29.5 °C), D_{H} continually increased, with a dramatic rise between 30.0 and 34.0 °C. The temperature dependence of D_{H} was in good agreement with the results of the transmittance measurement and the TEM investigation.

As indicated above, the LCST behavior of **1** derived from competition between two kinds of interactions: H-bonding between the surrounding water molecules and **1**, and intra- and intermolecular H-bonding interactions of **1**. Since both effects rely on interactions of the OEG chains, introduction of K^+ was expected to disrupt these phenomena by binding to the Tg groups.¹⁴ Preliminary investigations involved addition of an equimolar amount of KPF_6 to a D_2O solution of **1**. In the ^1H NMR spectrum, the proton signals of the benzyl (H_4) and glycol chains on **1** all showed slightly downfield shifts, indicating an interaction between K^+ and Tg chains (Figure S12). To get detailed information about the dependence of T_{cloud} on the molar ratio of **1** and K^+ , we investigated the aqueous solution properties by the cloud-point method. When the molar ratio of K^+ to **1** was changed from 0 to 1.1, T_{cloud} decreased from ~ 26.5 to ~ 24.5 °C (Figure 5a). T_{cloud} further decreased by another 1.00 °C when we adjusted the molar ratio to 1.2. Figure 5b shows that, with increasing molar ratio of K^+ to **1**, T_{cloud} decreased correspondingly. A possible explanation for this phenomenon is that, with

the introduction of additional K^+ , the complexation percentages of K^+ and Tg chains within a given metallacycle might increase accordingly. This increase could influence H-bonding between the surrounding water molecules and **1**, decreasing T_{cloud} .

In conclusion, a tri(ethylene glycol)-functionalized thermo-sensitive amphiphilic metallacycle **1** was prepared with high efficiency by means of the *directional-bonding approach*. It shows good LCST behavior, including both highly sensitive phase separation and excellent thermal reversibility. A stepwise decrease in [**1**] led to a sharp increase in T_{cloud} . Moreover, the turbidity temperature decreased with the introduction of K^+ . As such, the T_{cloud} of **1** was tunable by two methods, changing either the concentration of **1** or the molar ratio of K^+ to the amphiphilic metallacycle. Given the improved optical, magnetic, and electronic properties of supramolecular coordination complexes,^{12,13} diverse aggregates produced by macrocyclic amphiphiles,^{9c,d} and the favorable properties of emerging thermo-responsive materials,^{2–6} we expect that the fundamental results presented here will pave the way to construct novel multi-functional stimuli-responsive materials.

■ ASSOCIATED CONTENT

● Supporting Information

Experimental details and additional data. This material is available free of charge via the Internet at <http://pubs.acs.org>.

■ AUTHOR INFORMATION

Corresponding Authors

fhuang@zju.edu.cn

stang@chem.utah.edu

Notes

The authors declare no competing financial interest.

■ ACKNOWLEDGMENTS

F.H. thanks the National Basic Research Program (2013CB834502), the NSFC/China (21125417, 21434005), the State Key Laboratory of Chemical Engineering, and the Fundamental Research Funds for the Central Universities for financial support. P.J.S. thanks the NSF (1212799) for financial support. Dr. Xiaojie Cao from Research Center of Analysis and Measurement of Zhejiang University of Technology is thanked for her assistance with ESI-TOF-MS measurements.

■ REFERENCES

- (1) Cantor, C. R.; Schimmel, P. R. *Biophysical Chemistry*; W. H. Freeman and Co.: New York, 1980.
- (2) (a) Lachwa, J.; Szydłowski, J.; Visak, V. N.; Rebelo, L. P. N.; Seddon, K. R.; Ponte, M. N.; Esperanca, J. M. S. S. H.; Guedes, J. R. J. *Am. Chem. Soc.* **2005**, *127*, 6542–6543. (b) Jia, Z.; Chen, H.; Zhu, X.; Yan, D. *J. Am. Chem. Soc.* **2006**, *128*, 8144–8145. (c) Zhang, H.; Cooper, A. I. *Adv. Mater.* **2007**, *19*, 2439–2444. (d) Amajjahe, S.; Ritter, H. *Macromolecules* **2008**, *41*, 3250–3253. (e) Kabanov, A. V.; Vinogradov, S. V. *Angew. Chem., Int. Ed.* **2009**, *48*, 5418–5429. (f) Klaiherd, A.; Nagamini, C.; Thayumanavan, S. *J. Am. Chem. Soc.* **2009**, *131*, 4830–4838. (g) Wang, F.; Klaiherd, A.; Thayumanavan, S. *J. Am. Chem. Soc.* **2011**, *133*, 13496–13503. (h) Jochum, F. D.; Theato, P. *Chem. Soc. Rev.* **2012**, *42*, 7468–7483. (i) Ji, X.; Chen, J.; Chi, X.; Huang, F. *ACS Macro Lett.* **2014**, *3*, 110–113.
- (3) (a) Ito, T.; Hioki, T.; Yamaguchi, T.; Shinbo, T.; Nakao, S.; Kimura, S. *J. Am. Chem. Soc.* **2002**, *124*, 7840–7846. (b) Ito, T.; Sato, Y.; Yamaguchi, T.; Nakao, S. *Macromolecules* **2004**, *37*, 3407–3414. (c) Ding, Y.; Wang, Z.; Zhang, X. *Chem. Commun.* **2013**, *49*, 5580–5582.

- (4) (a) Kumar, S.; Dory, Y. L.; Lepage, M.; Zhao, Y. *Macromolecules* **2011**, *44*, 7385–7393. (b) Barroso, T.; Viveiros, R.; Temtem, M.; Casimiro, T.; Botelho do Rego, A. M.; Aguiar-Ricardo, A. *ACS Macro Lett.* **2012**, *1*, 356–360.

- (5) (a) Bhargava, P.; Tu, Y.; Zheng, J. X.; Xiong, H.; Quirk, R. P.; Cheng, S. Z. D. *J. Am. Chem. Soc.* **2007**, *129*, 1113–1121. (b) Zhang, L.; Guo, R.; Yang, M.; Jiang, X.; Liu, B. *Adv. Mater.* **2007**, *19*, 2988–2992. (c) Yhaya, F.; Lim, J.; Kim, Y.; Liang, M.; Gregory, A. M. *Macromolecules* **2011**, *44*, 8433–8445. (d) Wang, X.-J.; Xing, L.-B.; Wang, F.; Wang, G.-X.; Chen, B.; Tung, C.-H.; Wu, L.-Z. *Langmuir* **2011**, *27*, 8665–8671.

- (6) Koopmans, C.; Ritter, H. *J. Am. Chem. Soc.* **2007**, *129*, 3502–3503.

- (7) (a) Schild, H. G. *Prog. Polym. Sci.* **1992**, *17*, 163–249. (b) Wang, X. H.; Qiu, X. P.; Wu, C. *Macromolecules* **1998**, *31*, 2972–2976. (c) Maeda, Y.; Higuchi, T.; Ikeda, I. *Langmuir* **2000**, *16*, 7503–7509. (d) Ono, Y.; Shikata, T. *J. Am. Chem. Soc.* **2006**, *128*, 10030–10031. (e) Lutz, J.-F.; Akdemir, Ö.; Hoth, A. *J. Am. Chem. Soc.* **2006**, *128*, 13046–13407.

- (8) (a) Aathimankandan, S. V.; Savariar, E. N.; Thayumanavan, S. *J. Am. Chem. Soc.* **2005**, *127*, 14922–14929. (b) Hirose, T.; Matsuda, K.; Irie, M. *J. Org. Chem.* **2006**, *71*, 7499–7508. (c) Yang, W. Y.; Lee, E.; Lee, M. *J. Am. Chem. Soc.* **2006**, *128*, 3484–3485. (d) Betancourt, J. E.; Rivera, J. M. *J. Am. Chem. Soc.* **2009**, *131*, 16666–16668. (e) Lee, S.; Lee, J.-S.; Lee, C. H.; Jung, Y.-S.; Kim, J.-M. *Langmuir* **2011**, *27*, 1560–1564. (f) Dong, S.; Zheng, B.; Yao, Y.; Han, C.; Yuan, J.; Antonietti, M.; Huang, F. *Adv. Mater.* **2013**, *25*, 6864–6867.

- (9) (a) Ryu, J. H.; Oh, N. K.; Lee, M. *Chem. Commun.* **2005**, 1770–1772. (b) Seo, S. H.; Chang, J. Y.; Tew, G. N. *Angew. Chem., Int. Ed.* **2006**, *45*, 7526–7530. (c) Yao, Y.; Xue, M.; Chen, J.; Zhang, M.; Huang, F. *J. Am. Chem. Soc.* **2012**, *134*, 15712–15715. (d) Kauscher, U.; Stuart, M. C. A.; Drücker, P.; Galla, H.-J.; Ravoo, B. J. *Langmuir* **2013**, *29*, 7377–7383. (e) Yu, G.; Ma, Y.; Han, C.; Yao, Y.; Tang, G.; Mao, Z.; Gao, C.; Huang, F. *J. Am. Chem. Soc.* **2013**, *135*, 10310–10313.

- (10) (a) Chang, D. W.; Dai, L. *J. Mater. Chem.* **2007**, *17*, 364–371. (b) Lee, E.; Jeong, Y.-H.; Kim, J.-K.; Lee, M. *Macromolecules* **2007**, *40*, 8355–8360. (c) Li, W.; Zhang, A.; Chen, Y.; Feldman, K.; Wu, H.; Schlüter, A. D. *Chem. Commun.* **2008**, 5948–5950.

- (11) (a) Jun, Y. J.; Toti, U. S.; Kim, H. Y.; Yu, J. Y.; Jeong, B.; Jun, M. J.; Sohn, Y. S. *Angew. Chem., Int. Ed.* **2006**, *45*, 6173–6176. (b) Zhang, X.; Wang, C. *Chem. Soc. Rev.* **2011**, *40*, 94–101. (c) Li, L.; Che, Y.; Gross, D. E.; Huang, H.; Moore, J. S.; Zang, L. *ACS Macro Lett.* **2012**, *1*, 1335–1338. (d) Ogoshi, T.; Shiga, R.; Yamagishi, T.-a. *J. Am. Chem. Soc.* **2012**, *134*, 4577–4580. (e) Ogoshi, T.; Kida, K.; Yamagishi, T.-a. *J. Am. Chem. Soc.* **2012**, *134*, 20146–20150.

- (12) (a) Das, N.; Mukherjee, P. S.; Arif, A. M.; Stang, P. J. *J. Am. Chem. Soc.* **2003**, *125*, 13950–13951. (b) Mukherjee, P. S.; Das, N.; Kryshchenko, Y. K.; Arif, A. M.; Stang, P. J. *J. Am. Chem. Soc.* **2004**, *126*, 2464–2473. (c) Bar, A. K.; Gole, B.; Ghosh, S.; Mukherjee, P. S. *Dalton Trans.* **2009**, 6701–6704. (d) Chen, S.; Chen, L.-J.; Yang, H.-B.; Tian, H.; Zhu, W. *J. Am. Chem. Soc.* **2012**, *134*, 13596–13599. (e) Yan, X.; Jiang, B.; Cook, T. R.; Zhang, Y.; Li, J.; Yu, Y.; Huang, F.; Yang, H.-B.; Stang, P. J. *J. Am. Chem. Soc.* **2013**, *135*, 16813–16816. (f) Cook, T. R.; Zheng, Y.-R.; Stang, P. J. *Chem. Rev.* **2013**, *113*, 734–777. (g) Yan, X.; Li, S.; Pollock, J. B.; Cook, T. R.; Chen, J.; Zhang, Y.; Ji, X.; Yu, Y.; Huang, F.; Stang, P. J. *Proc. Natl. Acad. Sci. U.S.A.* **2013**, *110*, 15585–15590. (h) Chen, L.-J.; Zhao, G.-Z.; Jiang, B.; Sun, B.; Wang, M.; Xu, L.; He, J.; Abliz, Z.; Tan, H.; Li, X.; Yang, H.-B. *J. Am. Chem. Soc.* **2014**, *136*, 5993–6001. (i) Li, Z.-Y.; Zhang, Y.; Zhang, C.-W.; Chen, L.-J.; Wang, C.; Tan, H.; Yu, Y.; Li, X.; Yang, H.-B. *J. Am. Chem. Soc.* **2014**, *136*, 8577–8589.

- (13) (a) Munoz, M. J. M.; Fernández, G. *Chem. Sci.* **2012**, *3*, 1395–1398. (b) Yan, X.; Li, S.; Cook, T. R.; Ji, X.; Yao, Y.; Pollock, J. B.; Shi, Y.; Yu, G.; Li, J.; Huang, F.; Stang, P. J. *J. Am. Chem. Soc.* **2013**, *135*, 14036–14039.

- (14) (a) Gao, L.; Zheng, B.; Yao, Y.; Huang, F. *Soft Matter* **2013**, *9*, 7314–7319. (b) Terashima, T.; Kawabe, M.; Miyabara, Y.; Yoda, H.; Sawamoto, M. *Nat. Commun.* **2013**, *1*, 276–288.